

Novel Combretastatin Analogues Endowed with Antitumor Activity

Daniele Simoni,^{*,†} Romeo Romagnoli,[†] Riccardo Baruchello,[†] Riccardo Rondanin,[†] Michele Rizzi,[†] Maria Giovanna Pavani,[†] Domenico Alloati,[‡] Giuseppe Giannini,[‡] Marcella Marcellini,[‡] Teresa Riccioni,[‡] Massimo Castorina,[‡] Mario B. Guglielmi,[‡] Federica Bucci,[‡] Paolo Carminati,[‡] and Claudio Pisano^{*,‡}

Dipartimento di Scienze Farmaceutiche, Università di Ferrara, Via Fossato di Mortara 17/19, 44100 Ferrara, Italy, and R&D, Sigma-Tau Industrie Farmaceutiche Riunite S.p.A., Pomezia, Italy

Received October 24, 2005

We studied the anticancer activity of a series of new combretastatin derivatives with B-ring modifications. The structure–activity relationship (SAR) information confirmed the importance of cis-stereochemistry and of a phenolic moiety in B-ring. We selected the benzo[*b*]thiophene and benzofuran combretastatin analogues **11** (ST2151) and **13** (ST2179) and their phosphate prodrugs (**29** and **30**) for their high antitumor activity in *in vitro* and *in vivo* models. Cell exposure to IC₅₀ of **11**, **13**, and CA-4 led to the arrest of various cell types in the G₂/M phase of the cell cycle and induction of apoptosis. Mainly, **11** and **13** induced the formation of multinucleated cells with abnormal chromatin distribution, with only a minimal effect on the microtubule organization, with respect to CA-4. Interestingly, both the pharmacokinetic profile of **29** and its *in vivo* antitumor effect and those of **30**, active even after oral administration, suggest additional pharmacological differences between these compounds and CA-4P.

Introduction

Vascular targeting agents (VTAs) induce occlusion of pre-existing tumor blood vessels, producing tumor cell death from ischemia and extensive hemorrhagic necrosis.¹ The potential of vascular targeting as a therapeutic approach to cancer has been firmly established in several experimental studies.² In fact, preclinical studies show that VTAs exert an impressive antitumor activity when used as single chemotherapeutic agents.³ When combined, they enhance the effects of conventional chemotherapeutic agents⁴ such as radiation, hyperthermia, radioimmunotherapy, and antiangiogenic agents.^{5–8}

Combretastatin A-4 (CA-4, compound **1**), a natural stilbenoid isolated from *Combretum caffrum*, is a new VTA molecule known for its antitumor activity due to its anti-tubulin properties.^{9–15} The corresponding sodium phosphate prodrug (CA-4P, **2**) is water-soluble and currently showing promising results in phase I human cancer clinical trials.^{16,17} Moreover, other derivatives that carry the phosphate ester moiety are of particular interest in the quest for new anticancer drugs.^{18,19} In the case of CA-4, its structural simplicity, along with its ability to selectively damage tumor neovascularization, makes it very interesting from a medicinal chemistry point of view, stimulating the search for new and more potent compounds with improved pharmacological properties.²⁰ Previous structure–activity relationship (SAR) studies on CA-4 established that the cis-configuration of two benzene rings and methoxy groups at positions 3, 4, and 5 in the A-ring and at position 4 in the B-ring are essential for biological activity.²⁰

Recently, we started a study aimed at evaluating the apoptotic activity of natural and synthetic stilbenoids structurally related to CA-4.²¹ The alkenyl motif of CA-4 was replaced by five- and six-membered rings, leading in some cases to compounds with potent apoptotic activity. However, an investigation of cell cycle distribution and tubulin interaction suggested mechanisms not involving the mitotic spindle. Moreover, several publications

report that the B-ring of CA-4 can be replaced with naphthalene,²² quinoline, or a variety of six-membered heterocycles²⁰ (pyridine, pyrimidine, and pyridazine) without significant loss of antimetabolic and cytotoxic activity.

Therefore, in an ongoing project aimed at developing novel apoptosis inducer agents, we set out to study a novel class of stilbenes, structurally related to CA-4, focusing our attention on different ring modifications. Since the 3,4,5-trimethoxy substituent in the A-ring is essential for CA-4 activity, we maintained this substituted pattern throughout the present investigation, examining the effects due to replacement of the B-ring with different benzoheterocycles, obtaining a small library of novel combretastatins (Figure 1). We concentrated on benzofuran and benzothiophene rings as the most interesting substitutions but also synthesized indole, indazole, and naphthalene derivatives. An additional oxygenated function (methoxy or hydroxy) was always present and both *cis*- and *trans*-stereoisomers were obtained. Benzofuran and benzothiophene moieties have already been reported in the literature as bridge modifications of combretastatin-like derivatives maintaining the antitubulin activity.^{23,24}

After evaluation of a primary cytotoxicity screening, the most interesting derivatives were considered for further investigation. In particular, we selected the benzo[*b*]thiophene and the benzofuran molecules **11** (ST2151) and **13** (ST2179) and their phosphate prodrugs **29** (ST2495) and **30** (ST2496),²⁵ respectively (Table 1), for their high antitumor activity against different cancer models. A very important feature emerging from the detailed biological investigation into these compounds, reported here, is their potent antitumor activity, which could represent the basis for development of a novel chemotherapeutic drug.

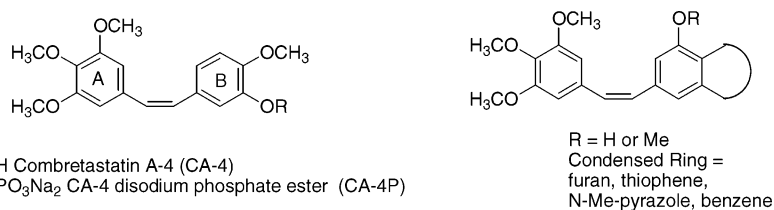
Chemistry

Scheme 1 outlines the synthetic route followed for the synthesis of the novel combretastatins (see Table 1). The heteroaromatic aldehydes **3a–j** (Figure 2) were transformed into the corresponding benzoheterocycles **4a–j** (Figure 3) by a Stobbe condensation using diethyl succinate, followed by cyclization as reported in the literature.²⁶ The phenol functions

* To whom correspondence should be addressed: Phone: +39-(0)532-291291. Fax: +39-(0)532-291296. E-mail: smd@unife.it.

[†] Università di Ferrara.

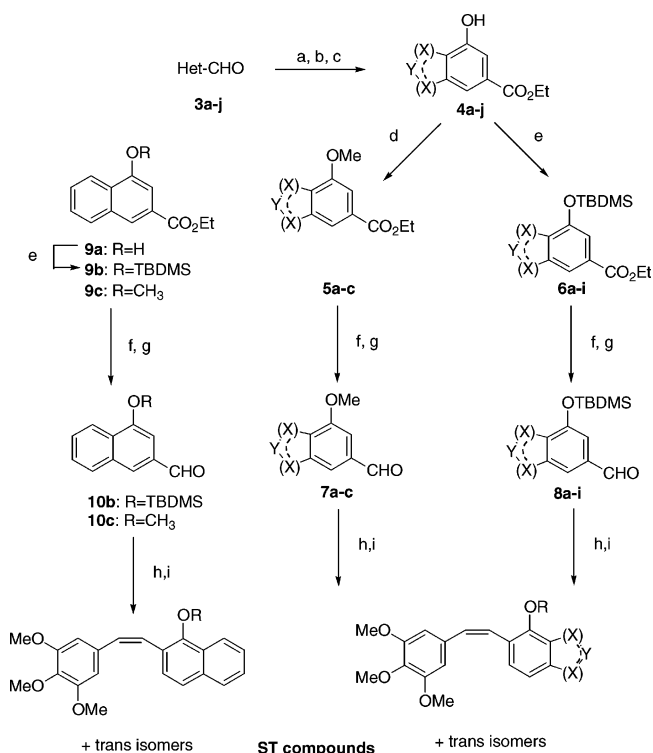
[‡] SIGMA-TAU Industrie Farmaceutiche Riunite S.p.A.

**Figure 1.** Natural and synthetic combretastatins.**Table 1.** IC₅₀ on BMEC Cell Line Determined for All New Combretastatin Derivatives^a

compd	B ring	X	E or Z	R	R ²	IC ₅₀ , μM
CA-4	A	-	Z	H	-	0.0037 ± 0.0003
CA-4P	A	-	Z	PO ₃ Na ₂	-	0.056 ± 0.0024
11	B	S	Z	H	H	0.087 ± 0.001
12	B	S	E	H	H	38.7 ± 9.6
13	B	O	Z	H	H	0.049 ± 0.001
14	B	O	E	H	H	27.7 ± 9.4
15	B	S	Z	H	2-CH ₃	0.023 ± 0.0074
16	B	S	E	H	2-CH ₃	0.84 ± 0.09
17	B	O	Z	H	2-CH ₃	0.093 ± 0.0069
18	B	O	E	H	2-CH ₃	12.3 ± 0.83
19	B	S	Z	H	3-phenyl	>2
20	B	S	E	H	3-phenyl	>20
21	B	O	Z	H	2-phenyl	>2
22	B	O	E	H	2-phenyl	>20
23	B	S	Z	H	2-phenyl	23 ± 3.2
24	B	S	E	H	2-phenyl	38 ± 4.5
25	B	S	Z	CH ₃	H	8.1 ± 0.3
26	B	S	E	CH ₃	H	53 ± 6.5
27	B	O	Z	CH ₃	H	7.5 ± 0.9
28	B	O	E	CH ₃	H	75 ± 6.7
29	B	S	Z	PO ₃ Na ₂	H	0.64 ± 0.04
30	B	O	Z	PO ₃ Na ₂	H	0.34 ± 0.01
31	C	S	Z	-	-	0.35 ± 0.02
32	C	S	E	-	-	24.8 ± 2.6
33	C	O	Z	-	-	0.054 ± 0.004
34	C	O	E	-	-	8.4 ± 1.6
35	D	-	Z	H	-	0.67 ± 0.045
36	D	-	E	H	-	56.4 ± 9.8
37	D	-	Z	CH ₃	-	10 ± 0.7
38	D	-	E	CH ₃	-	70 ± 10
39	E	-	Z	-	-	20 ± 6
40	E	-	E	-	-	32 ± 4
41	E	-	Z	-	-	0.028 ± 0.0055
42	E	-	E	-	-	1.9 ± 0.229

^a Cytotoxic activity was assayed by exposure for 24 h to substances and expressed as concentration required to inhibit tumor cell proliferation by 50% (IC₅₀). Data are expressed as mean ± SE from the dose-response curves of at least three independent experiments.

were protected with TBDMSCl, to give compounds **6a-i**, or methylated with dimethyl sulfate, to obtain compounds **5a-c**. Then, the carboxylic esters were converted into aldehydes **7a-c** and **8a-i** by reduction with LiAlH₄ and subsequent mild oxidation using MnO₂. Naphthalene aldehyde analogues **10b,c** were obtained similarly from the known esters **9a,c**,²⁷⁻²⁹ whose synthesis was also carried out by benzaldehyde using the above-

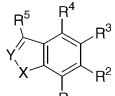
Scheme 1^a

^a Reagents and conditions: (a) (CH₂COOEt)₂, *t*-BuOH, KOBu, reflux, 2 h; (b) Ac₂O, AcONa, reflux, 5 h; (c) K₂CO₃, EtOH, reflux; (d) Me₂SO₄, K₂CO₃, THF; (e) imidazole, TBDMSCl, CH₂Cl₂; (f) LiAlH₄, THF; (g) MnO₂, CCl₄; (h) 3,4,5-trimethoxybenzyltriphenylphosphonium bromide, NaH, THF, 0 °C; (i) TBAF, CH₂Cl₂.

Compd.	X	Y	R	R ²	R ³
3a	S	CH	CHO	H	H
3b	O	CH	CHO	H	H
3c	S	CH	H	CHO	H
3d	O	CH	H	CHO	H
3e	N-CH ₃	N	H	CHO	H
3f	S	C-CH ₃	CHO	H	H
3g	O	C-CH ₃	CHO	H	H
3h	S	C-Ph	CHO	H	H
3i	O	C-Ph	CHO	H	H
3j	S	CH	CHO	H	C-Ph

Figure 2. Heterocyclic aldehydes as starting material in Scheme 1.

reported procedure. Finally, aldehydes **7a-c**, **8a-i**, **10b,c** and commercial indole-6-carbaldehyde were coupled with 3,4,5-trimethoxybenzyltriphenylphosphorane following a standard Wittig procedure. The phenolic moieties of the *E/Z* crude mixtures of silyl ethers were revealed by treatment with TBAF. The 1:1 mixture of the *Z* and *E* stilbene isomers was separated by silica gel column chromatography and the isomers identified



Compd.	X	Y	R	R ²	R ³	R ⁴	R ⁵
4a	S	CH	H	CO ₂ Et	H	OH	H
4b	O	CH	H	CO ₂ Et	H	OH	H
4c	S	CH	OH	H	CO ₂ Et	H	H
4d	O	CH	OH	H	CO ₂ Et	H	H
4e	N-CH ₃	N	OH	H	CO ₂ Et	H	H
4f	S	C-CH ₃	H	CO ₂ Et	H	OH	H
4g	O	C-CH ₃	H	CO ₂ Et	H	OH	H
4h	S	C-Ph	H	CO ₂ Et	H	OH	H
4i	O	C-Ph	H	CO ₂ Et	H	OH	H
4j	S	CH	H	CO ₂ Et	H	OH	Ph
5a	S	CH	H	CO ₂ Et	H	OCH ₃	H
5b	O	CH	H	CO ₂ Et	H	OCH ₃	H
5c	N-CH ₃	N	OCH ₃	H	CO ₂ Et	H	H
6a	S	CH	H	CO ₂ Et	H	OTBDMS	H
6b	O	CH	H	CO ₂ Et	H	OTBDMS	H
6c	S	CH	OTBDMS	H	CO ₂ Et	H	H
6d	O	CH	OTBDMS	H	CO ₂ Et	H	H
6e	S	C-CH ₃	H	CO ₂ Et	H	OTBDMS	H
6f	O	C-CH ₃	H	CO ₂ Et	H	OTBDMS	H
6g	S	C-Ph	H	CO ₂ Et	H	OTBDMS	H
6h	O	C-Ph	H	CO ₂ Et	H	OTBDMS	H
6i	S	CH	H	CO ₂ Et	H	OTBDMS	Ph
7a	S	CH	H	CHO	H	OCH ₃	H
7b	O	CH	H	CHO	H	OCH ₃	H
7c	N-CH ₃	N	OCH ₃	H	CHO	H	H
8a	S	CH	H	CHO	H	OTBDMS	H
8b	O	CH	H	CHO	H	OTBDMS	H
8c	S	CH	OTBDMS	H	CHO	H	H
8d	O	CH	OTBDMS	H	CHO	H	H
8e	S	C-CH ₃	H	CHO	H	OTBDMS	H
8f	O	C-CH ₃	H	CHO	H	OTBDMS	H
8g	S	C-Ph	H	CHO	H	OTBDMS	H
8h	O	C-Ph	H	CHO	H	OTBDMS	H
8i	S	CH	H	CHO	H	OTBDMS	Ph

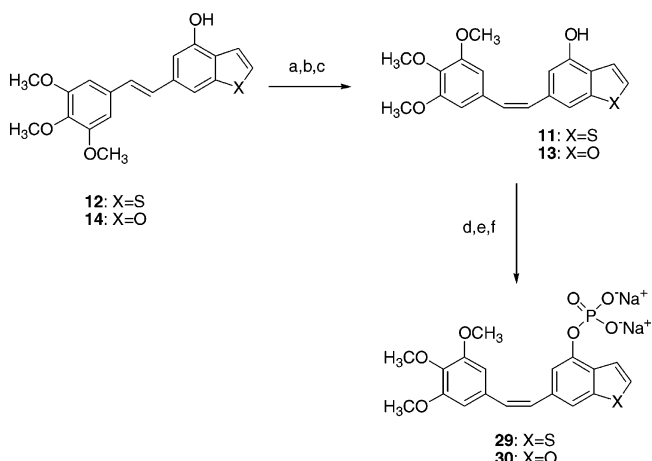
Figure 3. Synthetic intermediates as reported in Scheme 1.

by NMR for their different coupling constants between alkenyl proton signals (about 12 Hz for *Z*-isomers and 16 Hz for *E*-isomers).³⁰ Following initial results from biological assays, and in order to optimize the yield of the more active *cis* compounds, we exploited a photochemical isomerization³¹ that converted the *O*-acetylated *E*-isomers from **12** (ST2152) and **14** (ST2180)²⁵ into the corresponding *Z*-isomers; then, by detachment of the acetyl group with ethanolic K₂CO₃, we obtained the desired phenolic derivatives **11** and **13** (Scheme 2). In an attempt to prepare derivatives having enhanced aqueous solubility that can be more readily formulated, compounds **11** and **13** were transformed into the corresponding sodium phosphate prodrugs **29** and **30**, respectively, using a previously published three-step phosphorylation protocol.³²

Biological Results and Discussion

All the synthesized compounds were tested in a preliminary cytotoxicity assay on a BMEC cell line, the results being reported in Table 1. At first glance, it is evident that there is a difference in activity between *E*- and *Z*-stereoisomers, the latter being unambiguously more potent, which is unsurprising, since

Scheme 2^a



^a Reagents and conditions: (a) AcCl, C₅H₅N, CH₂Cl₂; (b) MeOH, mercury lamp; (c) K₂CO₃, EtOH, reflux; (d) (BnO)₂P(O)H, DIEA, CH₃CN, CCl₄, -25 °C; (e) TMSCl, NaI, CH₃CN; (f) NaOCH₃, CH₃OH.

Table 2. In Vitro Tubulin Polymerization Inhibition (TPI) and Colchicine Tubulin Binding Competition Assay (CTBC) of CA-4, **11**, and **13**

compd	IC ₅₀ ± SE (μM)	
	TPI	CTBC
CA-4	4.92 ± 0.2	0.0129 ± 0.009
11	24.6 ± 1.5	1.16 ± 0.0485
13	10.3 ± 0.05	2.5 ± 0.0796

it is well-documented in the literature.^{33,34} The phenolic moiety seems to have an important role in this class of compounds; indeed, the synthesized methoxy derivatives, **25** and **27**, demonstrated a dramatic loss of potency compared to their corresponding phenols, **11** and **13**. Furthermore, even the indolic *Z*-derivative, **41**, shows a very low IC₅₀, suggesting that another hydrogen-bond donor could replace the hydroxy group. In the hydroxylated benzofuran and benzothiophene series of derivatives, activity does not seem greatly influenced by the position of the endocyclic heteroatom (see **11–14** vs **31–34**).

Subsequently, in an effort to better understand the structure–activity relationships of this class of derivatives, we studied the influence of a substituent at the 2- and 3-positions of the heterocyclic system of compounds **15–24**, through alteration of its steric bulk, seeking a potentially positive lipophilic interaction capable of enhancing the observed activities. The synthesized series, with a methyl or phenyl group at the said positions, offered the interesting information (Table 1) that methyl derivatives **15** and **17** show almost unchanged activity compared to **11** and **13**. On the contrary, a phenyl ring, either at the 2- or 3-position (compounds **19**, **21**, and **23**), causes an important loss of potency. Thus, only small substituents seem to be allowed for the 2- and 3-positions, in some cases showing slight improvement in activity.

Among synthesized compounds we selected two new molecules, **11** and **13**, and their phosphate prodrugs, **29** and **30**, respectively, for their antitumor activity in different cancer models. Preliminary screening was carried out, analyzing the activity of the new compounds in both in vitro tubulin polymerization inhibition (TPI) and colchicine tubulin binding competition assay (CTBC). The results show that **11** and **13** determine a relatively lower inhibition of tubulin polymerization compared to that of CA-4 (Table 2). On the other hand, **11** and **13** show a 100–200-fold reduction in affinity to the colchicine binding site compared to CA-4.

Table 3. Antiproliferative Effect of CA-4, CA-4P, **11**, **13**, and Their Phosphate Prodrugs against the Proliferation of Several Cell Lines^a

cell line	cell type	IC ₅₀ (nM)					
		CA-4	CA-4P	11	29	13	30
HUVEC	human endothelium	1.5 ± 0.4	34 ± 0.34	49 ± 0.64	83 ± 2.06	31 ± 1.7	85 ± 1.2
H460	human lung carcinoma	1.24 ± 0.02	37 ± 1	74 ± 2.9	620 ± 65	53 ± 1.3	780 ± 3.4
HCT116	human colon carcinoma	1.9 ± 0.01	16 ± 0.13	84 ± 3.8	3000 ± 102	54 ± 9	1680 ± 70
MeWo	human melanoma	4 ± 0.0001	10 ± 1.2	68 ± 5	830 ± 0.13	71 ± 17	820 ± 77
MCF-7	human breast carcinoma	2 ± 0.064	23 ± 1.1	66 ± 2.7	639 ± 21	38 ± 3	646 ± 29
MCF-7 dx	human breast carcinoma	2.3 ± 0.018	9.4 ± 21	54 ± 2.1	487 ± 14.8	28 ± 0.5	357 ± 9.4
A2780	human ovarian carcinoma	2.19 ± 0.08	nd	70 ± 2	500 ± 20	50 ± 2	260 ± 6
A2780 dx	doxorubicin-resistant human ovarian carcinoma	1.66 ± 0.1	22 ± 0.6	95 ± 7	750 ± 50	46 ± 4.4	290 ± 16
IGROV-1	human ovarian carcinoma	10.3 ± 0.55	nd	280 ± 4	1610 ± 67	110 ± 6	680 ± 60

^a Cytotoxic activity was assayed by exposure for 24 h to substances and expressed as concentration required to inhibit tumor cell proliferation by 50% (IC₅₀). Data are expressed as mean ± SE from the dose–response curves of at least three independent experiments; nd = not determined.

Table 4. Effects of CA-4, **11**, and **13** on Cell Cycle

	G _{1/0} (%)	S (%)	G _{2/M} (%)	Apo (%)
24-h treatment				
untreated	46	29	26	0
CA-4	8	12	79	19
11	16	27	57	40
13	8	25	67	26
24-h treatment + 24-h recovery				
untreated	58	29	13	0
CA-4	62	22	16	30
11	36	38	27	30
13	13	43	44	24
24-h treatment + 48-h recovery				
untreated	76	13	11	0
CA-4	55	18	27	47
11	57	13	30	40
13	52	22	26	35

The lower antitubulin activity of **11** and **13** correlates well with their reduced cytotoxic potency with respect to CA-4. In fact, although **11** and **13** determine cell growth inhibition in various cell lines, their IC₅₀ is about 20 to 50 times higher than that of reference compound CA-4 (Tables 1 and 3). The phosphate prodrugs **29** and **30** are 10–20 times less active than their respective drugs in all cell lines, except for HUVEC, in which the activity is only two times lower and similar to that of CA-4P. This unexpected result might be related to a rapid formation in HUVEC conditioned medium of more active compounds **11** and **13** from phosphate hydrolysis of their prodrugs **29** and **30**. Alternatively, **29** and **30** might be intrinsically more active against human endothelial cell with respect to tumor cell lines.

The 4-methoxy Z-isomers **25** and **27**, along with all E-isomers, show dramatic reduction in cytotoxicity (IC₅₀ > 5 μM, data not shown) when tested on endothelial cells. These results indicate that substitution of the 4-hydroxy with a 4-methoxy group is detrimental to cytotoxic activity.

To compare the effects of both **11** and **13** on the cell cycle with those of CA-4, NCI-H460 cells were exposed to the various molecules for 24 h and allowed to recover in drug-free medium for a further 24 and 48 h. There is a quite similar perturbation of cell cycle progression in the H460 cell line after treatment with equitoxic concentrations of **11** (160 nM), **13** (100 nM), and CA-4 (3 nM), corresponding to their respective IC₈₀ values (Table 4). In these cells, there is an increase of sub-G₁ cells, consistent with the occurrence of apoptotic DNA fragmentation. In addition, after 24-h treatment and during the next 48 h following drug removal, there is a persistent accumulation of cells in G_{2/M} phases.

In an attempt to identify the cellular effects that may be relevant to the antiproliferative activity of **11** and **13**, we

evaluated their activity on the alteration of the microtubule network by tubulin immunostaining, comparing it to that of CA-4. To this end, we added the drugs to human endothelial cells (HUVEC) and human lung carcinoma cells (H460) at different concentrations for 24 h. As expected, tubulin immunostaining reveals that cells exposed to CA-4 at IC₅₀, as well as at IC₈₀ (data not shown), produce complete disruption of the microtubule structure in endothelial and tumor cells, compared to untreated cells (Figure 4, panels A, B). Instead of the clear antimicrotubule effect of CA-4, **11** and **13** determine, at their IC₅₀ and IC₈₀ levels, the formation of giant aberrant multinucleated cells with abnormal chromatin distribution and a mild effect on microtubule organization.

Further analysis, by counting the number of nuclei per cell, reveals that 24-h exposition to IC₈₀ of **11** and **13** in H460 cells induces a significant 40–50% of multinucleated cells (*p* < 0.0001 vs control, Figure 5). This phenomenon is less evident in cells treated with equitoxic concentrations of CA-4 (IC₈₀) and becomes more relevant only when starting from higher concentrations (2 × IC₈₀) of the molecule (*p* < 0.0001 vs control). The peculiar cell phenotype, induced by **11** and **13** treatment, is retained by their prodrugs **29** and **30**, when used at the equitoxic concentration of parental compounds (data not shown).

To investigate the antitumor activity of these compounds in vivo, we first analyzed the pharmacokinetic behavior of compound **29** (**11** phosphate prodrug). After single intravenous administration of compound **29** to healthy mice (100 mg/kg iv), plasma samples were collected over 24 h and the plasma concentrations of compounds **29** and **11** were simultaneously determined by HPLC. Table 5 presents the pharmacokinetic parameters, while Figure 6 shows the mean profile of plasma levels. Plasma concentrations of both compounds are not measurable 24 h after treatment. The apparent terminal elimination half-life (*t*_{1/2}) of compound **29** is 1.32 h, similar to that described for CA-4P,³⁵ and there is a similar *t*_{1/2} (1.72 h) for compound **11**. However, the plasma concentrations of the more active compound **11** (AUC_{0–t_z} = 5.00 μg·h/mL) are approximately 39 times lower than those for the prodrug **29** (AUC_{0–t_z} = 282.43 μg·h/mL), thus suggesting that the release kinetics of **11** from **29** differ from those of CA-4P to CA-4.³⁴

In the in vivo experiments, **29** and **30**, administered intravenously at a dose of 60 mg/kg (q2dx6), produce the same antitumor effects as the same CA-4P dose and schedule in a human non-small lung cancer model (H460) xenografted in nude mice (Figure 7). Interestingly, **29** and **30** significantly reduce tumor growth even when administered orally (60 mg/kg; bid, qdx5x3w).

In conclusion, in an effort to obtain novel derivatives of natural combretastatin A-4, we synthesized and tested a series

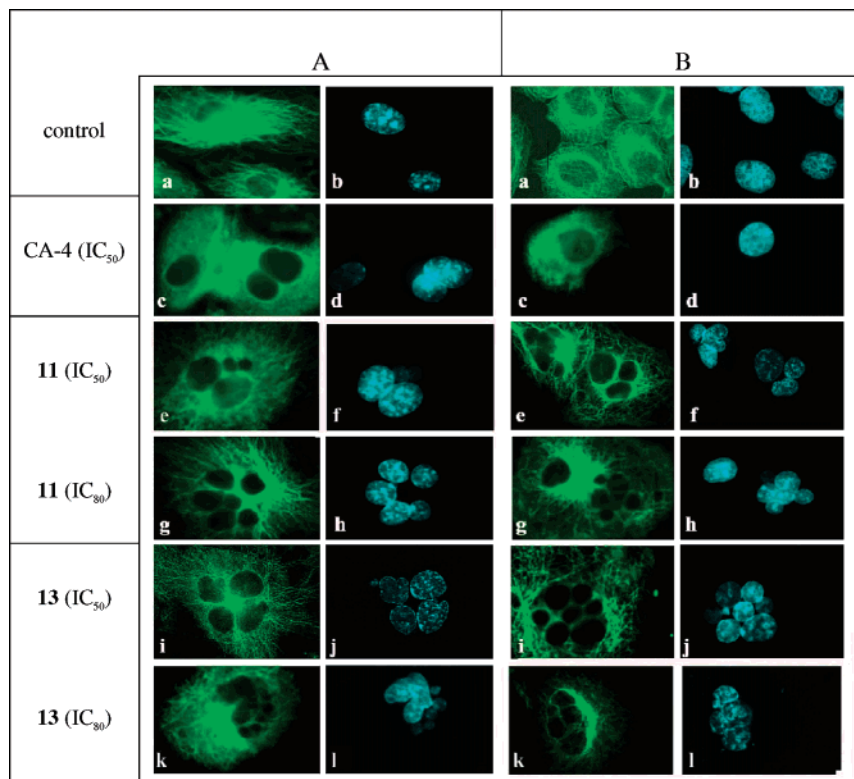


Figure 4. HUVEC (panel A) and H460 cells (panel B) were exposed at different concentrations of drugs (brackets) for 24 h and immunostained with mAb anti- α -tubulin (sigma) as shown in a–k and with Hoechst to stain nuclei b–l.

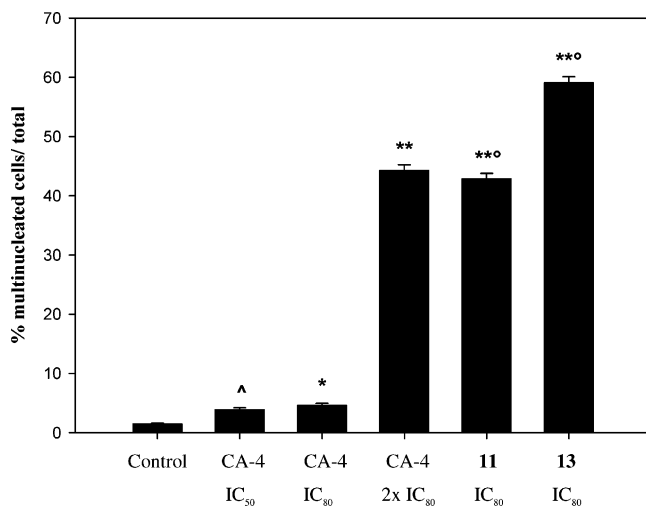


Figure 5. Evaluation of multinucleated cells after 24-h exposure to CA-4, **11**, and **13**. Values are mean \pm SD from two independent experiments. $\wedge p = 0.07$, $*p < 0.05$, $**p < 0.0001$ vs control; $^{\circ}p < 0.0001$ compared to CA-4 IC₈₀ treatment (two-tailed Student's *t*-test).

of compounds modified at the B-ring. Several aromatic and heteroaromatic rings were introduced, bearing an oxygenated appendage. Our results suggest that benzofuran and benzothiophene may be considered interesting compounds for the development of potent antitumoral CA-4 derivatives. Furthermore, a hydroxylated function always produced higher activity than did the corresponding methoxyl group. A hydrophobic substitution at the 2- or 3-position of the heterocycle moiety was tolerated only by the addition of a little steric bulk. All trans isomers are definitely less active than the corresponding cis isomers.

Concerning the in vitro results, we suggest that the tumor cell lines treated with **11** and **13** undergo cell death mainly through mitotic catastrophe, as demonstrated by the presence

Table 5. Pharmacokinetic Parameters of Compounds **29** and **11** in Female Mice after Intravenous Bolus Injection of Prodrug **29** (100 mg/kg)

parameters ^a	29	11
C_0 ($\mu\text{g/mL}$)	778.88	0
C_{max} ($\mu\text{g/mL}$)	319.60	8.16
t_{max} (h)	0.25	0.25
t_z (h)	8	8
$t_{1/2}$ (h)	1.32	1.72
AUC_{0-t_z} ($\mu\text{g h/mL}$)	282.43	5.00
$\text{AUC}_{0-\infty}$ ($\mu\text{g h/mL}$)	282.63	5.02

^a C_0 , initial plasma concentration obtained by extrapolation to time 0; C_{max} , highest measured concentration corresponding to t_{max} ; t_{max} , time of the maximum observed concentration; t_z , time of last measurable concentration; $t_{1/2}$, apparent terminal elimination half-life; AUC_{0-t_z} , area under the plasma concentration–time curve up to time t_z ; $\text{AUC}_{0-\infty}$, area under the plasma concentration–time curve extrapolated to infinity.

of giant multinucleated cells. On the contrary, this pattern was specular to that obtained by equal pharmacological active concentrations of CA-4, which is characterized mostly by microtubules damage. These observations suggest that the activity of **11** and **13** might not be related solely to a microtubule-damaging mechanism and that an additional mechanism(s) involved in mitosis control should be considered.

Interestingly, pharmacokinetic studies reveal that only a small fraction of the more active drug **11** forms from compound **29**. Since **29** is as active on human endothelial cells as **11**, it is argued that both compounds may act as an antivascular agent. Alternatively, the activity of **29** is realized through a complex profile of metabolites (including **11**) that can be produced after intravenous injection of the prodrug, as described in the literature for CA-4P.

Materials and Methods

Chemistry. Melting points were obtained with a Kofler apparatus and are uncorrected. Reaction courses and product mixtures were routinely monitored by thin-layer chromatography (TLC) on Merck

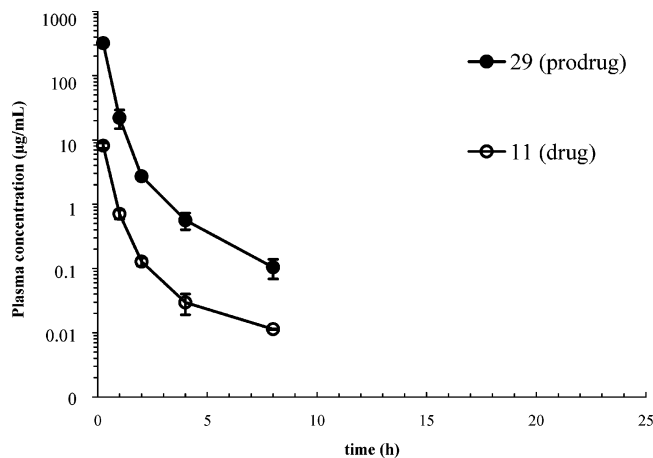


Figure 6. Mean profile (\pm SEM; $n = 3$) of **29** and **11** plasma levels ($\mu\text{g/mL}$) in female mice after intravenous bolus injection of prodrug **29** (100 mg/kg).

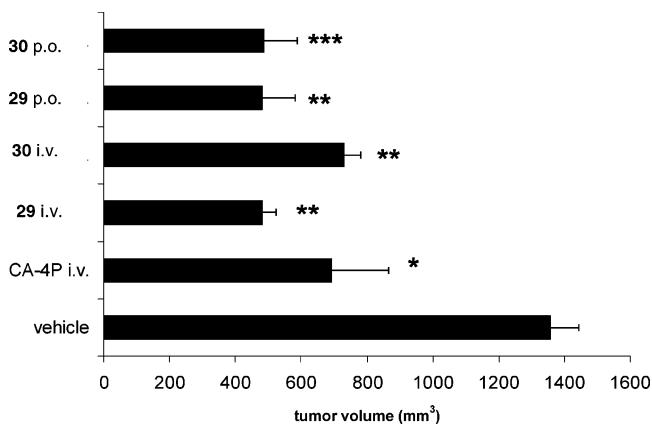


Figure 7. Antitumor activity of CA-4P, **29**, and **30** on human NCI-H460 lung carcinoma. Tumor volume was determined on day 20 after tumor cell injection. Values represent mean \pm SD from two independent experiments. * $p < 0.05$, ** $p < 0.01$, *** $p < 0.001$ vs control. Neither mortality nor reduction of body weight was observed.

precoated silica gel F₂₅₄ plates. Nuclear magnetic resonance (¹H and ¹³C NMR) spectra were determined, with a Bruker AC-200 spectrometer, and peak positions are given in parts per million downfield from tetramethylsilane as internal standard. Mass spectra were obtained with a Bruker Daltonics MALDI-TOF (Omniflex mod.). Photoisomerization was performed with a medium-pressure mercury Hanau TQ 120 K lamp.

All drying operations were performed over anhydrous sodium sulfate. Column chromatography (medium pressure) was carried out with 60–200 mesh silica gel, using the flash technique. Yields were given after chromatographic purification. Pure samples were obtained after recrystallization from 2-propanol. Microanalysis of all new synthesized compounds agreed within $\pm 0.4\%$ of calculated values.

General Procedure for the Synthesis of Stilbenes 11–28 and 31–42. 3,4,5-Trimethoxybenzyltriphenylphosphonium bromide (2 mmol, 1.05 g, 2 equiv) was added to a solution of aldehyde (**7a–c**, **8a–i**, or **10b,c**, 2 mmol) in 10 mL of anhydrous THF. The suspension thus obtained was cooled in an ice bath and then NaH (50% in mineral suspension, 2.2 mmol, 1.1 equiv., 110 mg) was added. The reaction was stirred at room temperature for 24 h, filtered on a Celite bed, and washed with THF. After solvent evaporation, the residue was extracted with methylene chloride (15 mL), washed with water (5 mL) and brine (5 mL), dried, and evaporated again.

For derivatives in which the phenolic moiety is protected as the TBDMS ether, the residue was dissolved in methylene chloride (10 mL) and tetrabutylammonium fluoride (6 mmol, 3 equiv) was

added. After 1 h at room temperature, the solution was diluted with methylene chloride (5 mL), washed with water (3×5 mL) and brine (5 mL), and dried (Na_2SO_4). After concentration, the residue was purified by flash chromatography on silica gel.

Starting from **8a** the following compounds were produced.

6-[(Z)-2-(3,4,5-Trimethoxyphenyl)ethenyl]benzo[b]thiophen-4-ol (11). Yield: 41% (280 mg), colorless solid. Mp: 145–147 °C. ¹H NMR (CDCl_3) δ : 3.64 (s, 6H), 3.83 (s, 3H), 5.34 (s, 1H), 6.50 (d, $J = 12.6$ Hz, 1H), 6.54 (s, 1H), 6.60 (d, $J = 12.6$ Hz, 1H), 6.69 (s, 1H), 7.27 (s, 1H), 7.32 (d, $J = 5.6$ Hz, 1H), 7.41 (d, $J = 5.6$ Hz, 1H), 7.42 (s, 1H). ¹³C NMR (CDCl_3) δ : 56.0, 106.3, 109.5, 115.8, 119.8, 125.5, 129.6, 130.3, 153.0. Anal. ($\text{C}_{19}\text{H}_{18}\text{O}_4\text{S}$) C, H, S.

6-[(E)-2-(3,4,5-Trimethoxyphenyl)ethenyl]benzo[b]thiophen-4-ol (12). Yield: 43% (295 mg), yellow solid. Mp: 67–69 °C. ¹H NMR (CDCl_3) δ : 3.88 (s, 6H), 3.92 (s, 3H), 5.50 (s, 1H), 6.74 (s, 2H), 6.93 (s, 1H), 7.03 (s, 2H), 7.35 (d, $J = 5.2$ Hz, 1H), 7.43 (d, $J = 5.2$ Hz, 1H), 7.56 (s, 1H). ¹³C NMR (CDCl_3) δ : 56.2, 61.1, 103.6, 106.6, 114.1, 119.9, 125.5, 128.1, 128.8, 129.1, 133.2, 135.2, 137.9, 142.4, 150.8, 153.5. Anal. ($\text{C}_{18}\text{H}_{19}\text{O}_4\text{S}$) C, H, S.

Starting from **8b** the following compounds were produced.

6-[(Z)-2-(3,4,5-Trimethoxyphenyl)ethenyl]benzofuran-4-ol (13). Yield: 34% (220 mg), colorless solid that solidifies at 4 °C. Mp: 134–136 °C. ¹H NMR (CDCl_3) δ : 3.64 (s, 6H), 3.83 (s, 3H), 5.94 (s, 1H), 6.73 (s, 2H), 6.82 (d, $J = 6.0$ Hz, 1H), 6.85 (d, $J = 2.2$ Hz, 1H), 6.99 (s, 2H), 7.24 (d, $J = 6.0$ Hz, 1H), 7.55 (d, $J = 2.2$ Hz, 1H). ¹³C NMR (CDCl_3) δ : 55.9, 61.0, 103.5, 105.2, 106.1, 108.6, 115.9, 129.8, 130.1, 132.5, 134.6, 144.3, 148.8, 152.9, 156.8. Anal. ($\text{C}_{19}\text{H}_{18}\text{O}_5$) C, H.

6-[(E)-2-(3,4,5-Trimethoxyphenyl)ethenyl]benzofuran-4-ol (14). Yield: 37% (240 mg), light yellow solid. Mp: 142–143 °C. ¹H NMR (CDCl_3) δ : 3.89 (s, 6H), 3.92 (s, 3H), 5.50 (s, 1H), 6.74 (s, 2H), 6.93 (s, 1H), 7.03 (s, 2H), 7.35 (d, $J = 5.2$ Hz, 1H), 7.43 (d, $J = 5.2$ Hz, 1H), 7.56 (s, 1H). Anal. ($\text{C}_{19}\text{H}_{18}\text{O}_5$) C, H.

Starting from **8e** the following compounds were produced.

6-[(Z)-2-(3,4,5-Trimethoxyphenyl)ethenyl]-2-methylbenzo[b]thiophen-4-ol (15). Yield: 31% (220 mg), colorless solid. Mp: 118–120 °C. ¹H NMR (CDCl_3) δ : 2.56 (s, 3H), 3.65 (s, 6H), 3.84 (s, 3H), 5.20 (br, 1H), 6.47 (d, $J = 12$ Hz, 1H), 6.54 (s, 2H), 6.57 (d, $J = 12$ Hz, 1H), 6.64 (d, $J = 0.8$ Hz, 1H), 7.03 (d, $J = 2$ Hz, 1H), 7.30 (s, 1H). ¹³C NMR (CDCl_3) δ : 16.2, 55.9, 60.9, 103.4, 106.0, 109.5, 115.4, 117.4, 128.2, 129.6, 129.8, 132.5, 133.7, 137.2, 140.1, 141.1, 152.9. MALDI-TOF: 357.6 [M⁺]. Anal. ($\text{C}_{20}\text{H}_{20}\text{O}_4\text{S}$) C, H, S.

6-[(E)-2-(3,4,5-Trimethoxyphenyl)ethenyl]-2-methylbenzo[b]thiophen-4-ol (16). Yield: 33% (235 mg), colorless solid. Mp: 200–202 °C. ¹H NMR (CDCl_3) δ : 2.59 (s, 3H), 3.87 (s, 3H), 3.92 (s, 6H), 5.18 (br, 1H), 6.73 (s, 2H), 6.89 (s, 1H), 7.0 (s, 2H), 7.04 (d, $J = 12$ Hz, 1H), 7.45 (s, 1H). ¹³C NMR (CDCl_3) δ : 16.3, 56.2, 61.1, 103.5, 106.8, 113.7, 117.4, 128.2, 128.4, 140.3, 149.9, 153.5, 207.2. MALDI-TOF: 356.6 [M⁺]. Anal. ($\text{C}_{20}\text{H}_{20}\text{O}_4\text{S}$) C, H, S.

Starting from **8f** the following compounds were produced.

6-[(Z)-2-(3,4,5-Trimethoxyphenyl)ethenyl]-2-methylbenzofuran-4-ol (17). Yield: 29% (195 mg), colorless solid. Mp: 114–116 °C. ¹H NMR (CDCl_3) δ : 2.42 (s, 3H), 3.65 (s, 6H), 3.84 (s, 3H), 5.18 (s, 1H), 6.38 (s, 1H), 6.47 (d, $J = 12$ Hz, 1H), 6.53 (s, 2H), 6.57–6.60 (m, 2H), 6.97 (d, $J = 1.2$ Hz, 1H). ¹³C NMR (75 MHz, CDCl_3) δ : 14.0, 55.9, 60.9, 99.4, 104.4, 106.1, 108.5, 117.4, 129.4, 130.1, 132.7, 133.2, 137.0, 148.0, 152.8, 154.7, 156.3. MALDI-TOF: 340.6 [M⁺]. Anal. ($\text{C}_{20}\text{H}_{20}\text{O}_5$) C, H.

6-[(E)-2-(3,4,5-Trimethoxyphenyl)ethenyl]-2-methylbenzofuran-4-ol (18). Yield: 33% (225 mg), colorless solid. Mp: 65–70 °C. ¹H NMR (CDCl_3) δ : 2.46 (s, 3H), 3.87 (s, 3H), 3.92 (s, 6H), 4.98 (br, 1H), 6.41 (s, 1H), 6.97 (d, $J = 16.6$ Hz, 1H), 7.01 (d, $J = 16.6$ Hz, 1H), 7.16 (s, 1H), 6.57–6.60 (m, 2H), 6.97 (d, $J = 1.2$ Hz, 1H). ¹³C NMR (75 MHz, CDCl_3) δ : 14.2, 56.2, 61.1, 99.5, 102.6, 103.5, 106.1, 118.1, 128.0, 128.5, 133.3, 133.9, 148.3, 153.5, 155.1, 156.8. MALDI-TOF: 340.6 [M⁺]. Anal. ($\text{C}_{20}\text{H}_{20}\text{O}_5$) C, H.

Starting from **8i** the following compounds were produced.

6-[(Z)-2-(3,4,5-Trimethoxyphenyl)ethenyl]-3-phenylbenzo[b]thiophen-4-ol (19). Yield: 36% (300 mg), oil. ¹H NMR (CDCl_3)

δ : 3.66 (s, 6H), 3.84 (s, 3H), 5.21 (br, 1H), 6.62 (d, $J = 12.4$ Hz, 1H), 6.57 (s, 2H), 6.62 (d, $J = 12.4$ Hz, 1H), 6.79 (d, $J = 1.2$ Hz, 1H), 7.14 (s, 1H), 7.45 (m, 1H), 7.50–7.52 (m, 4H). ^{13}C NMR (CDCl_3) δ : 16.2, 55.9, 60.9, 103.4, 106.0, 109.5, 115.4, 117.4, 128.2, 129.6, 129.8, 132.5, 133.7, 137.2, 140.1, 141.1, 152.9. MALDI-TOF: 418.1 [M+]. Anal. ($\text{C}_{25}\text{H}_{22}\text{O}_4\text{S}$) C, H, S.

6-[(E)-2-(3,4,5-Trimethoxyphenyl)ethenyl]-3-phenylbenzo[b]-thiophen-4-ol (20). Yield: 40% (335 mg), colorless solid. Mp: 138–140 °C. ^1H NMR (CDCl_3) δ : 3.88 (s, 3H), 3.93 (s, 6H), 5.34 (s, 1H), 6.76 (s, 2H), 7.02 (d, $J = 1.2$ Hz, 1H), 7.05 (d, $J = 16$ Hz, 1H), 7.10 (d, $J = 16$ Hz, 1H), 7.16 (s, 1H), 7.48–7.56 (m, 5H), 7.58 (d, $J = 1.2$ Hz, 1H). ^{13}C NMR (CDCl_3) δ : 20.6, 56.2, 61.1, 103.6, 108.2, 114.0, 123.8, 127.8, 128.8, 129.1, 129.3, 129.5, 133.1, 135.9, 153.5. MALDI-TOF: 418.2 [M+]. Anal. ($\text{C}_{25}\text{H}_{22}\text{O}_4\text{S}$) C, H, S.

Starting from **8h** the following compounds were produced.

6-[(Z)-2-(3,4,5-Trimethoxyphenyl)ethenyl]-2-phenylbenzofuran-4-ol (21). Yield: 27% (215 mg), colorless solid. Mp: 60–62 °C. ^1H NMR (CDCl_3) δ : 3.67 (s, 6H), 3.85 (s, 3H), 5.13 (br, 1H), 6.51 (d, $J = 12$ Hz, 1H), 6.55 (s, 2H), 6.60 (d, $J = 12$ Hz, 1H), 6.62 (s, 1H), 7.05 (d, $J = 1.2$ Hz, 1H), 7.32–7.36 (m, 1H), 7.41–7.46 (m, 3H), 7.81–7.84 (m, 2H). ^{13}C NMR (CDCl_3) δ : 56.0, 61.0, 98.3, 105.1, 106.1, 108.9, 123.8, 117.9, 124.8, 128.6, 128.9, 129.9, 130.0, 148.6, 152.9, 156.5. MALDI-TOF: 401.9 [M+]. Anal. ($\text{C}_{25}\text{H}_{22}\text{O}_5$) C, H.

6-[(E)-2-(3,4,5-Trimethoxyphenyl)ethenyl]-2-phenylbenzofuran-4-ol (22). Yield: 35% (280 mg), colorless solid. Mp: 180–182 °C. ^1H NMR (CDCl_3) δ : 3.89 (s, 3H), 3.93 (s, 6H), 5.18 (br, 1H), 6.75 (s, 2H), 6.84 (d, $J = 0.8$ Hz, 1H), 7.03 (s, 2H), 7.08 (d, $J = 0.8$ Hz, 1H), 7.28 (s, 1H), 7.34–7.37 (m, 1H), 7.44–7.47 (m, 2H), 7.84–7.86 (m, 2H). ^{13}C NMR (CDCl_3) δ : 56.2, 62.1, 98.4, 102.9, 103.6, 106.5, 124.8, 128.4, 128.9, 130.3, 149.9, 153.5. MALDI-TOF: 401.9 [M+]. Anal. ($\text{C}_{25}\text{H}_{22}\text{O}_5$) C, H.

Starting from **8g** the following compounds were produced.

6-[(Z)-2-(3,4,5-Trimethoxyphenyl)ethenyl]-2-phenylbenzo[b]-thiophen-4-ol (23). Yield: 31% (260 mg), oil. ^1H NMR (CDCl_3) δ : 3.60 (s, 6H), 3.78 (s, 3H), 5.22 (br, 1H), 6.44 (d, $J = 12.4$ Hz, 1H), 6.50 (s, 2H), 6.55 (d, $J = 12.4$ Hz, 1H), 6.61 (s, 1H), 7.27–7.40 (m, 4H), 7.57–7.66 (m, 3H). MALDI-TOF: 418 [M+]. Anal. ($\text{C}_{25}\text{H}_{22}\text{O}_4\text{S}$) C, H, S.

6-[(E)-2-(3,4,5-Trimethoxyphenyl)ethenyl]-2-phenylbenzo[b]-thiophen-4-ol (24). Yield: 30% (250 mg), colorless solid. Mp: 218–220 °C. ^1H NMR (CDCl_3) δ : 3.88 (s, 3H), 3.93 (s, 6H), 5.32 (br, 1H), 6.75 (s, 2H), 6.95 (s, 1H), 7.04 (s, 1H), 7.33–7.37 (m, 2H), 7.42–7.46 (m, 2H), 7.65 (s, 1H), 7.66 (s, 1H), 7.70–7.73 (m, 2H). MALDI-TOF: 418 [M+]. Anal. ($\text{C}_{25}\text{H}_{22}\text{O}_4\text{S}$) C, H, S.

Starting from **7a** the following compounds were produced.

4-Methoxy-6-[(Z)-2-(3,4,5-trimethoxyphenyl)ethenyl]benzo[b]-thiophene (25). Yield: 42% (300 mg), yellow oil. ^1H NMR (CDCl_3) δ : 3.65 (s, 6H), 3.76 (s, 3H), 3.84 (s, 3H), 6.55 (s, 1H), 6.58 (d, $J = 11.2$ Hz, 1H), 6.64 (d, $J = 11.2$ Hz, 1H), 6.70 (s, 1H), 7.27 (s, 1H), 7.31 (d, $J = 5.0$ Hz, 1H), 7.42 (d, $J = 5.0$ Hz, 1H), 7.44 (s, 1H). MALDI-TOF: 356.4 [M + 1]. Anal. ($\text{C}_{20}\text{H}_{20}\text{O}_4\text{S}$) C, H, S.

4-Methoxy-6-[(E)-2-(3,4,5-trimethoxyphenyl)ethenyl]benzo[b]-thiophene (26). Yield: 44% (315 mg), yellow solid; mp 171–173 °C. ^1H NMR (CDCl_3) δ : 3.89 (s, 6H), 3.94 (s, 3H), 4.03 (s, 3H), 6.78 (s, 2H), 6.95 (s, 1H), 7.10 (s, 2H), 7.33 (d, $J = 5.6$ Hz, 1H), 7.47 (d, $J = 5.6$ Hz, 1H), 7.58 (s, 1H). MALDI-TOF: 356.3 [M + 1]. Anal. ($\text{C}_{20}\text{H}_{20}\text{O}_4\text{S}$) C, H, S.

Starting from **7b** the following compounds were produced.

4-Methoxy-6-[(Z)-2-(3,4,5-trimethoxyphenyl)ethenyl]benzofuran (27). Yield: 38% (260 mg), yellow oil. ^1H NMR (CDCl_3) δ : 3.65 (s, 6H), 3.74 (s, 3H), 3.83 (s, 3H), 6.52 (s, 1H), 6.55 (d, $J = 11.2$ Hz, 1H), 6.62 (d, $J = 11.2$ Hz, 1H), 6.63 (s, 1H), 6.80 (s, 1H), 7.27 (s, 1H), 7.10 (s, 1H), 7.51 (s, 1H). MALDI-TOF: 340.6 [M + 1]. Anal. ($\text{C}_{20}\text{H}_{20}\text{O}_5$) C, H.

4-Methoxy-6-[(E)-2-(3,4,5-trimethoxyphenyl)ethenyl]benzofuran (28). Yield: 41% (280 mg), yellow solid. Mp: 152–153 °C. ^1H NMR (CDCl_3) δ : 3.88 (s, 6H), 3.94 (s, 3H), 4.00 (s, 3H), 6.76 (s, 2H), 6.84 (s, 2H), 7.08 (s, 2H), 7.28 (d, $J = 2.2$ Hz, 1H),

7.54 (d, $J = 2.2$ Hz, 1H). MALDI-TOF: 340.6 [M + 1]. Anal. ($\text{C}_{20}\text{H}_{20}\text{O}_5$) C, H.

Starting from **8c** the following compounds were produced.

5-[(Z)-2-(3,4,5-Trimethoxyphenyl)ethenyl]benzo[b]thiophen-7-ol (31). Yield: 31% (210 mg), brown solid. Mp: 152–154 °C; ^1H NMR (CDCl_3) δ : 3.63 (s, 6H), 3.83 (s, 3H), 5.51 (s, 1H), 6.48 (d, $J = 12.2$ Hz, 1H), 6.52 (s, 1H), 6.64 (d, $J = 12.2$ Hz, 1H), 6.73 (s, 1H), 7.26 (s, 1H), 7.29 (d, $J = 3.2$ Hz, 1H), 7.41 (d, $J = 3.2$ Hz, 1H), 7.43 (s, 1H). Anal. ($\text{C}_{19}\text{H}_{18}\text{O}_4\text{S}$) C, H, S.

5-[(E)-2-(3,4,5-Trimethoxyphenyl)ethenyl]benzo[b]thiophen-7-ol (32). Yield: 38% (260 mg), yellow solid. Mp: 172–174 °C; ^1H NMR (CDCl_3) δ : 3.89 (s, 6H), 3.92 (s, 3H), 5.63 (s, 1H), 6.74 (s, 2H), 6.94 (s, 1H), 7.02 (d, $J = 2.8$ Hz, 1H), 7.32 (d, $J = 5.2$ Hz, 1H), 7.45 (d, $J = 5.2$ Hz, 1H), 7.53 (s, 1H). Anal. ($\text{C}_{19}\text{H}_{18}\text{O}_4\text{S}$) C, H, S.

Starting from **8d** the following compounds were produced.

5-[(Z)-2-(3,4,5-Trimethoxyphenyl)ethenyl]benzofuran-7-ol (33). Yield: 36% (235 mg), colorless solid. Mp: 140–141 °C; ^1H NMR (CDCl_3) δ : 3.63 (s, 6H), 3.83 (s, 3H), 5.33 (s, 1H), 6.46 (d, $J = 12.4$ Hz, 1H), 6.52 (s, 1H), 6.57 (d, $J = 12.4$ Hz, 1H), 6.69 (d, $J = 2.2$ Hz, 1H), 6.82 (s, 1H), 7.12 (s, 1H), 7.26 (s, 1H), 7.58 (d, $J = 2.2$ Hz, 1H). ^{13}C NMR (CDCl_3) δ : 55.9, 61.0, 106.2, 107.3, 111.4, 114.4, 129.1, 129.5, 130.0, 132.6, 133.3, 137.2, 140.7, 145.4, 152.9. Anal. ($\text{C}_{19}\text{H}_{18}\text{O}_5$) C, H.

5-[(E)-2-(3,4,5-Trimethoxyphenyl)ethenyl]benzofuran-7-ol (34). Yield: 42% (275 mg), colorless solid. Mp: 173–175 °C; ^1H NMR (CDCl_3) δ : 3.89 (s, 6H), 3.92 (s, 3H), 6.01 (s, 1H), 6.74 (s, 2H), 6.97 (s, 1H), 7.06 (d, $J = 3.2$ Hz, 1H), 7.26 (d, $J = 5.2$ Hz, 1H), 7.45 (d, $J = 5.2$ Hz, 1H), 7.60 (s, 1H). ^{13}C NMR (CDCl_3) δ : 56.2, 61.1, 103.5, 107.5, 108.5, 112.1, 128.0, 128.5, 129.4, 133.3, 133.8, 137.8, 141.1, 143.3, 145.5, 153.5. Anal. ($\text{C}_{19}\text{H}_{18}\text{O}_5$) C, H.

Starting from **10b** the following compounds were produced.

3-[(Z)-2-(3,4,5-Trimethoxyphenyl)ethenyl]naphthalen-1-ol (35). Yield: 33% (220 mg), yellow solid. Mp: 163–165 °C; ^1H NMR (CDCl_3) δ : 3.62 (s, 6H), 3.84 (s, 3H), 5.56 (s, 1H), 6.53 (d, $J = 12.4$ Hz, 1H), 6.56 (s, 2H), 6.68 (d, $J = 12.4$ Hz, 1H), 6.79 (s, 1H), 7.38 (s, 1H), 7.45 (m, 2H), 7.72 (dd, $J = 9.8$ and 3.6 Hz, 1H), 8.11 (dd, $J = 9.8$ and 3.6 Hz, 1H).

3-[(E)-2-(3,4,5-Trimethoxyphenyl)ethenyl]naphthalen-1-ol (36). Yield: 40% (270 mg), yellow solid. Mp: 176–178 °C; ^1H NMR (CDCl_3) δ : 3.90 (s, 3H), 3.93 (s, 6H), 5.73 (s, 1H), 6.77 (s, 2H), 7.07 (m, 3H), 7.46 (m, 3H), 7.80 (dd, $J = 9.6$ and 2.8 Hz, 1H), 8.14 (dd, $J = 9.6$ and 2.8 Hz, 1H).

Starting from **10c** the following compounds were produced.

1-Methoxy-3-[(Z)-2-(3,4,5-trimethoxyphenyl)ethenyl]naphthalene (37). Yield: 36% (250 mg), oil. ^1H NMR (CDCl_3) δ : 3.63 (s, 6H), 3.75 (s, 3H), 3.83 (s, 3H), 6.57 (s, 1H), 6.66 (d, $J = 13.2$ Hz, 1H), 6.71 (d, $J = 13.2$ Hz, 1H), 6.75 (s, 1H), 7.44 (m, 4H), 7.69 (m, 1H), 8.12 (m, 1H). MALDI-TOF: 350.3 [M + 1].

1-Methoxy-3-[(E)-2-(3,4,5-trimethoxyphenyl)ethenyl]naphthalene (38). Yield: 40% (280 mg), yellow solid. Mp: 166–168 °C. ^1H NMR (CDCl_3) δ : 3.89 (s, 3H), 3.95 (s, 6H), 4.09 (s, 3H), 6.80 (s, 2H), 7.06 (s, 1H), 7.16 (s, 2H), 7.46 (m, 3H), 7.76 (dd, $J = 9.2$ and 1.8 Hz, 1H), 8.20 (dd, $J = 9.2$ and 1.8 Hz, 1H). MALDI-TOF: 350.3 [M + 1].

Starting from **7c** the following compounds were produced.

7-Methoxy-1-methyl-5-[(Z)-2-(3,4,5-trimethoxyphenyl)ethenyl]-1H-indazole (39). Yield: 29% (205 mg), colorless solid. Mp: 182–183 °C; ^1H NMR (CDCl_3) δ : 3.64 (s, 3H), 3.67 (s, 3H), 3.82 (s, 3H), 4.23 (s, 3H), 6.51 (d, $J = 12.5$ Hz, 1H), 6.53 (s, 2H), 6.59 (d, $J = 12.5$ Hz, 1H), 7.19 (s, 1H), 7.80 (s, 2H).

7-Methoxy-1-methyl-5-[(E)-2-(3,4,5-trimethoxyphenyl)ethenyl]-1H-indazole (40). Yield: 35% (250 mg), oil. ^1H NMR (CDCl_3) δ : 3.86 (s, 3H), 3.91 (s, 6H), 4.01 (s, 3H), 4.28 (s, 3H), 6.73 (s, 2H), 6.94 (d, $J = 15.8$ Hz, 1H), 7.06 (d, $J = 15.8$ Hz, 1H), 7.31 (s, 1H), 7.86 (s, 2H).

Starting from commercial indole-6-carboxaldehyde the following compounds were produced.

6-[(Z)-2-(3,4,5-Trimethoxyphenyl)ethenyl]-1H-indole (41). Yield: 18% (110 mg), oil. ^1H NMR (CDCl_3) δ : 3.60 (s, 6H), 3.83 (s, 3H), 6.43–6.51 (m, 2H), 6.53 (s, 2H), 6.70 (d, $J = 12.2$ Hz,

1H), 7.10 (dd, $J = 8.2$ Hz, 1.2 Hz, 1H), 7.16–7.19 (m, 1H), 7.33 (s, 1H), 7.51 (d, $J = 8.2$ Hz, 1H), 8.09 (br, 1H). ^{13}C NMR (CDCl_3) δ : 55.9, 61.0, 102.7, 106.0, 111.4, 120.3, 121.5, 124.9, 128.7, 131.2, 133.2, 152.9. MALDI-TOF: 309.3 [M⁺]. Anal. ($\text{C}_{19}\text{H}_{19}\text{NO}_3$) C, H.

6-[(E)-2-(3,4,5-Trimethoxyphenyl)ethenyl]-1H-indole (42). Yield: 28% (175 mg), oil. ^1H NMR (CDCl_3) δ : 3.87 (s, 3H), 3.92 (s, 6H), 6.74 (s, 2H), 6.84 (d, $J = 0.8$ Hz, 1H), 7.03 (s, 2H), 7.08 (d, $J = 0.8$ Hz, 1H), 7.28 (s, 1H), 7.34–7.37 (m, 1H), 7.44–7.47 (m, 2H), 7.84–7.86 (m, 2H), 8.21 (br, 1H). ^{13}C NMR (CDCl_3) δ : 56.2, 62.1, 98.4, 102.9, 103.6, 106.5, 124.8, 128.4, 128.9, 130.3, 149.9, 153.5. MALDI-TOF: 309.2 [M⁺]. Anal. ($\text{C}_{19}\text{H}_{19}\text{NO}_3$) C, H.

General Procedure for the Synthesis of Phosphate Prodrugs 29 and 30. CCl_4 (580 μL , 6 mmol, 5 equiv) was added to a solution of 1.2 mmol of compound **11** or **13** in 5 mL of anhydrous CH_3CN cooled to -25°C . After approximately 10 min, 440 μL (2.52 mmol, 2.1 equiv) of diisopropylethylamine, 15 mg (0.12 mmol, 0.1 equiv) of (dimethylamino)pyridine, and 380 μL (1.74 mmol, 1.45 equiv) of dibenzyl phosphate were added to the solution. After 2 h at -10°C , when the reaction was completed, 20 mL of KH_2PO_4 (0.5 M) was added and the aqueous phase was extracted with ethyl acetate (3 \times 10 mL). The organic phases were dried over anhydrous Na_2SO_4 , and the crude intermediate product was purified by chromatography.

NaI (36 mg, 2.4 mmol, 2 equiv) and 300 μL (2.4 mmol, 2 equiv) of Me_3SiCl dissolved in 1 mL of anhydrous CH_3CN were added at room temperature to a solution of 1.2 mmol of dibenzyl ester dissolved in 7 mL of anhydrous CH_3CN . After 2 h, when the reaction was completed, a small amount of water was added to dissolve the salts. A solution of 10% $\text{Na}_2\text{S}_2\text{O}_3$ was added until decolorization of the reaction mixture. The solution thus obtained was extracted with ethyl acetate, the organic phases were dried over Na_2SO_4 , and solvent was removed in vacuo. The crude oil obtained was dissolved in 4 mL of anhydrous MeOH , and 130 mg (2.4 mmol, 2 equiv) of NaOMe was added to the solution. The mixture was left to stand at room temperature for 20 h. Then, solvent was removed in vacuo and the residue washed with Et_2O to give the desired product.

Starting from **11** the following compounds were produced.

6-[(Z)-2-(3,4,5-Trimethoxyphenyl)ethenyl]-1-benzo[b]thiophen-4-ol 4-O-Dibenzyl Phosphate. The product was purified by flash chromatography on silica gel using hexane:ethyl acetate 8:2. Yield: 86% (625 mg), yellow oil. ^1H NMR (CDCl_3) δ : 3.6 (s, 6H), 3.8 (s, 3H), 5.05 (s, 2H), 5.1 (s, 2H), 6.5 (s, 2H), 6.6 (bs, 2H), 7.2–7.4 (m, 11H), 7.6 (s, 1H). ^{13}C NMR (CDCl_3) δ : 56.1, 61.1, 70.3, 106.4, 115.9, 119.7, 120.4, 127.1, 128.2, 128.8, 128.9, 129.0, 131.1, 131.6, 132.2, 134.9, 135.6, 153.2. MS-IS: [M + H]⁺ = 603.2. Anal. ($\text{C}_{33}\text{H}_{31}\text{O}_7\text{PS}$) C, H.

Disodium 6-[(Z)-2-(3,4,5-Trimethoxyphenyl)ethenyl]-1-benzothiofen-4-ol 4-O-Phosphate (29). Yield: 92% (515 mg), colorless solid. Mp: 226°C . ^1H NMR (D_2O) δ : 3.57 (s, 6H), 3.75 (s, 3H), 6.50 (d, $J = 12.1$ Hz, 1H), 6.63 (s, 2H), 6.74 (d, $J = 12.1$ Hz, 1H), 7.30 (d, $J = 5.5$ Hz, 1H), 7.39 (s, 1H), 7.57 (s, 1H), 7.66 (d, $J = 5.5$ Hz, 1H). ^{13}C NMR (D_2O) δ : 54.4, 59.2, 105.7, 113.8, 121.2, 122.8, 128.5, 129.9, 131.6, 131.8, 132.5, 134.1, 136.3, 139.7, 150.1, 150.2, 152.1. MS-IS: [M – 1][–] = 419. Anal. ($\text{C}_{19}\text{H}_{17}\text{Na}_2\text{O}_7\text{PS}$) C, H, S.

Starting from **13** the following compounds were produced.

6-[(Z)-2-(3,4,5-Trimethoxyphenyl)ethenyl]-1-benzofuran-4-ol 4-O-Dibenzyl Phosphate. The product was purified by flash chromatography on silica gel using hexane:ethyl acetate 7:3. Yield: 88% (620 mg), yellow oil. ^1H NMR (CDCl_3) δ : 3.6 (s, 6H), 3.8 (s, 3H), 5.05 (s, 2H), 5.1 (s, 2H), 6.45 (s, 2H), 6.55 (bs, 2H), 6.75 (bs, 1H), 7.05 (s, 1H), 7.2–7.4 (m, 11H), 7.5 (bs, 1H). ^{13}C NMR (CDCl_3) δ : 56.1, 61.1, 70.3, 98.8, 104.3, 106.4, 109.1, 115.1, 119.9, 128.2, 128.8, 128.9, 129.2, 130.9, 132.3, 134.7, 135.5, 145.5, 153.2, 156.5. MS-IS: [M + H]⁺ = 587.2. Anal. ($\text{C}_{33}\text{H}_{31}\text{O}_8\text{P}$) C, H.

Disodium 6-[(Z)-2-(3,4,5-Trimethoxyphenyl)ethenyl]-1-benzofuran-4-ol 4-O-Phosphate (30). Yield: 91% (490 mg), colorless

solid. Mp: 212°C . ^1H NMR (CD_3OD) δ : 3.60 (s, 6H), 3.76 (s, 3H), 6.48 (d, $J = 12.1$ Hz, 1H), 6.61 (s, 2H), 6.73 (d, $J = 12.1$ Hz, 1H), 7.00 (s, 1H), 7.04 (d, $J = 2.2$ Hz, 1H), 7.44 (s, 1H), 7.53 (d, $J = 2.2$ Hz, 1H). ^{13}C NMR (D_2O) δ : 54.4, 59.2, 103.2, 104.3, 105.6, 113.3, 118.9, 119.1, 128.2, 130.2, 132.7, 133.5, 136.3, 142.8, 148.4, 148.5, 152.1, 155.5. MS-IS [M – 1][–] = 403. Anal. ($\text{C}_{19}\text{H}_{17}\text{Na}_2\text{O}_8\text{P}$) C, H, S.

General Procedure for Photochemical Isomerization. Step 1: Acetylation of E-Isomers. Acetyl chloride (1.8 mL, 20 mmol) was added to an ice-cooled solution of *E*-isomer **12** or **14** (10 mmol) dissolved in methylene chloride (20 mL) containing pyridine (1.6 mL, 20 mmol) and the mixture stirred until completion of reaction (10 min). Water (10 mL) was added, the organic layer was separated, washed with saturated aqueous NaHCO_3 , and dried. The solvent was evaporated to give a residue, which was purified by silica gel column chromatography.

4-Acetyloxy-6-[(E)-2-(3,4,5-trimethoxyphenyl)ethenyl]benzo[b]thiophene. Yield: 71% (2.73 g), colorless solid. Mp: 136 – 138°C . ^1H NMR (CDCl_3) δ : 2.43 (s, 3H), 3.89 (s, 6H), 3.92 (s, 3H), 6.69 (d, $J = 1.4$ Hz, 1H), 6.78 (s, 2H), 7.03 (s, 2H), 7.19 (s, 1H), 7.50 (s, 1H), 7.60 (d, $J = 1.4$ Hz, 1H).

4-Acetyloxy-6-[(E)-2-(3,4,5-trimethoxyphenyl)ethenyl]benzofuran. Yield: 74% (2.73 g), yellow oil. ^1H NMR (CDCl_3) δ : 2.41 (s, 3H), 3.88 (s, 6H), 3.92 (s, 3H), 6.67 (d, $J = 1.2$ Hz, 1H), 6.75 (s, 2H), 7.06 (s, 2H), 7.23 (s, 1H), 7.52 (s, 1H), 7.61 (d, $J = 1.2$ Hz, 1H).

Step 2: Irradiation. A stirred solution of the *O*-acetyl derivatives (1 mmol) dissolved in 300 mL of MeOH was irradiated with a mercury lamp for 2 h. After removal of the methanol in vacuo, the product was purified by silica gel column chromatography.

4-Acetyloxy-6-[(Z)-2-(3,4,5-trimethoxyphenyl)ethenyl]benzo[b]thiophene. The unreacted starting material *E*-isomer (32%) and the corresponding *Z*-isomer (64%, 245 mg) were separated by silica gel column chromatography to give a brown oil. ^1H NMR (CDCl_3) δ : 2.20 (s, 3H), 3.63 (s, 6H), 3.82 (s, 3H), 6.51 (s, 2H), 6.58 (d, $J = 12.2$ Hz, 1H), 6.92 (s, 1H), 6.98 (s, 2H), 7.30 (s, 1H), 7.58 (d, $J = 2.0$ Hz, 1H).

4-Acetyloxy-6-[(Z)-2-(3,4,5-trimethoxyphenyl)ethenyl]benzofuran. The unreacted *E*-isomer (24%) and the corresponding *Z*-isomer (67%, 250 mg) were separated by silica gel column chromatography to give a yellow oil. ^1H NMR (CDCl_3) δ : 2.18 (s, 3H), 3.65 (s, 6H), 3.84 (s, 3H), 6.50 (s, 2H), 6.58 (d, $J = 6.0$ Hz, 1H), 6.96 (s, 1H), 6.99 (s, 2H), 7.34 (s, 1H), 7.58 (d, $J = 2.0$ Hz, 1H).

Step 3: Hydrolysis of Z-Acetyl Derivatives. Compounds **11** (63% yield) and **13** (72% yield) were obtained following the *O*-deacetylation method reported in the general procedure for the synthesis of **4a–j**.

Biology. Cell Culture and Cytotoxicity Assay. Primary cultures of bovine microvascular endothelial cells (BMEC) were obtained from bovine adrenal glands as described by Folkman.³⁶ BMEC were maintained in DMEM supplemented with 20% fetal calf serum (FCS), 50 units/mL heparin (Sigma, St. Louis, MO), 50 $\mu\text{g}/\text{mL}$ bovine brain extract, and 100 units/mL gentamycin.

HUVEC (human umbilical vein endothelial cells) were obtained from BioWhittaker (Walkersville, MD) and grown in EGM-2 (BioWhittaker). The following cell lines were purchased from ATCC and cultured according to manufacturer's instructions: NCI-H460 human non-small cell lung carcinoma, MCF-7 human hormone-dependent breast carcinoma, and MeWo human melanoma. Wild-type and doxorubicin-resistant A2780 ovarian carcinoma and doxorubicin-resistant MCF-7 (both gifts of Dr. F. Zunino, Istituto Nazionale dei Tumori, Milan, Italy) were grown in RPMI 1640 containing 10% FBS and 50 $\mu\text{g}/\text{mL}$ gentamycin sulfate. IGROV-1 ovarian carcinoma cells, also obtained from Dr. Zunino, were cultured in D-MEM containing 10% FBS. HCT-116 human colon carcinoma cells, purchased from "Istituto Zooprofilattico" (Brescia, Italy), were grown in McCoy's medium containing 10% FBS and 50 $\mu\text{g}/\text{mL}$ gentamycin sulfate.

To test the effect of the drugs on cell growth, the above cell lines were resuspended at different concentrations in 200 μL of

appropriate growth medium and seeded in 96-well plates. Twenty-four hours after plating, scalar concentrations of each drug were added to the cells. The drugs were removed after 24 h and, after a further 48 h of recovery, the number of surviving cells was determined by staining with sulforhodamine B test, as previously described.³⁷ Optical density was measured at 564 nm. Results, expressed as concentrations that inhibit 50% of cell growth (IC₅₀), were calculated by the ALLFIT program.

Tubulin Polymerization Inhibition. The tubulin polymerization test was performed by CytoDINAMIX Screen (Cytoskeleton Inc., Denver, CO). One hundred microliters of 3 mg/mL HTS tubulin in G-PEM buffer plus 5% glycerol at 4 °C was pipetted into wells of the 96-well plate and incubated at 37 °C in the presence or absence of single compounds. Tubulin polymerization was detected by measuring the absorbance of the solution (340 nm) for 60 min. Because the amount of tubulin polymerized is directly proportional to the AUC (area under the curve), we used AUC to determine the concentration that inhibited tubulin polymerization by 50% (IC₅₀).³⁸ The AUC of the untreated control was set to 100% polymerization (maximal attainable polymerization), and the IC₅₀ was calculated by nonlinear regression.

Colchicine Tubulin Binding Competition. Competition-binding SPAs (Scintillation Proximity Assay) were conducted in 96-well plates. Radiolabeled [³H]colchicine (final concentration 0.08 μM), unlabeled compound, and 0.5 mg of special long-chain biotin-labeled tubulin (Cytoskeleton, Denver, CO) were incubated together in 100 μL of binding buffer [80 mM PIPES, 1 mM EGTA, 1 mM MgCl₂, 1 mM GTP (pH 6.8)] for 2 h at 37 °C. Streptavidin-labeled yttrium SPA beads (80 μg suspended in 20 μL of binding buffer; Amersham, Arlington Heights, IL) were added to each well, and the bound radioactivity was determined using a scintillation counter. Nonspecific binding was determined in the presence of excess unlabeled colchicines. The IC₅₀ was calculated as the concentration of compounds required for 50% inhibition of [³H]colchicine-binding; each data point is a result of the average of triplicate wells and analyzed by nonlinear regression analysis with the Prism GraphPad software program.

Cell Cycle. NCI-H460 cells were exposed to the various molecules (at the IC₈₀ dose) for 24 h and allowed to recover in drug-free medium for 24 and 48 h. Cells were then harvested with trypsin/EDTA, pooled with the respective supernatant, and fixed in cold 70% ethanol at 4 °C. On the day of analysis, ethanol was removed, cells were treated with RNase (75 kU/mL) for 30 min at 37 °C, and propidium iodide (PI) was added (50 μg/mL) to stain cellular DNA. Samples (2 × 10⁴ cells) were processed by a FACScan flow cytometer to assess cell cycle distribution and apoptosis (Apo). Apo was evaluated by measuring the percentage of cells with hypodiploid DNA content (sub-G_{1/0} population) with CELLQuest software, while cell cycle analysis was performed with ModFit software.

Immunofluorescence. For tubulin immunostaining, the cells, cultured on gelatin-coated cover slips, were treated with the compounds at their respective IC₅₀, 2 × IC₅₀, and 4 × IC₅₀ values. After 24 h the cells were washed with PBS and then fixed in cold methanol for 5 min and acetone for 1 min. Then, the fixed cells were incubated in a PBS solution containing 0.1% Triton X-100 and 0.5% acetic acid for 10 min and, after three washings in PBS, in a solution containing 2 μg/mL of the monoclonal anti- α -tubulin antibody (Sigma Chemicals Co., St. Louis, MO) for 1 h at room temperature in a humidified chamber. Following primary antibody incubation, the cells were washed three times in PBS and incubated with an AlexaFluor-conjugated goat anti-mouse secondary antibody (Molecular Probes, Leiden, The Netherlands) at a concentration of 20 μg/mL for 1 h at room temperature, in the dark. For nuclear staining, cells were incubated with Hoechst 33342 (Sigma Chemicals) at a concentration of 10 μg/mL for 10 min at room temperature, in the dark. Cover slips were then mounted with 50% glycerol in PBS. Cells were analyzed with an epifluorescent microscope (Polyvar, Zeiss AG, Germany) and imaged with a cooled CCD camera (Photometrics, Roper Scientific Inc., CA). Images were then processed with Metamorph software (Universal

Imaging, Downingtown, PA). Quantification of multinucleated cells was performed by counting cells containing more than two nuclei (including micronuclei) in 20 randomly chosen microscope fields at 100×. These counts were expressed as percentage of the total α -tubulin stained cells in identical fields.

In Vivo Study. For the in vivo xenograft model, 3.0 × 10⁶ NCI-H460 cells, resuspended in 100 μL of Ca²⁺/Mg²⁺-free Hank's balanced solution (HBSS), were inoculated subcutaneously into the right flank of CD-1 nude female mice. Five days after cell injection, tumors attained a mass of about 30 mg and the mice were assigned to treatment groups, eight mice per group. Animals were treated with **29** and **30** either orally (po), at a dose of 60 mg/kg twice a day, 5 days a week over a three-week period (qdx5x3w), or intravenously (iv) at the same dose of 60 mg/kg every other day for a total of six administrations (q2dx6). Control groups received CA-4P at a dose of 60 mg/kg iv (q2dx6) or were treated with vehicle only. Animals were size-matched for palpable tumors (20–30 mm³) and tumor size was measured twice a week with a Vernier caliper. Tumor volume (TV, mm³) was estimated by the formula: length × (width)²/2, where width and length are the shortest and longest diameters of each tumor, respectively. When tumors reached a mass of about 1.4 g, mice were sacrificed. Toxicity of the different drug treatments was determined as body weight loss percentage (% max BWL) = 100 – (mean BW_x/mean BW₁ × 100), where BW_x is the mean BW at the day of maximal loss during treatment and BW₁ is the mean BW on the first day of treatment.

The care and husbandry of animals were in accordance with European Directives 86/609 and with the Italian Regulatory system (D.L. vol. 116, Art. 6, 27 Jan 1992). Statistical comparison of data was performed by the nonparametric Mann–Whitney *U* test. Probability values of *p* ≤ 0.05 were considered significant. Dixon's test was eventually used for exclusion of abnormal values at the end of treatment.

In Vivo Pharmacokinetics. Healthy CD-1 female mice (three mice/group) were treated with 100 mg/kg of **29** by intravenous bolus as a 5% glucose solution. Blood samples were taken at various time points up to 24 h postdose from the retro-orbital plexus under terminal anesthesia and collected in Eppendorf tubes containing 2% EDTA. Plasma was separated immediately by centrifugation at 1000g at 4 °C for 10 min and deproteinized by adding two volumes of methanol kept at –20 °C. Samples were placed on ice for 10 min, followed by centrifugation at 10 000g at 4 °C for 10 min, and transferred into vials for high-performance liquid chromatography (HPLC). This method permitted the simultaneous extraction of the phosphate prodrug **29** and of the corresponding water-insoluble combretastatin analogue **11**. Indeed, the estimated recovery factor (*R*) was 96 ± 3% for **29** and 80 ± 7% for **11**, evaluated by adding primary stock solutions of the compounds, respectively, in water or methanol containing up to 2% DMSO to untreated plasma sample processed as described. Concentrations of **29** and **11** were calculated from the respective calibration curves, which were linear over the range tested (from 0.0624 to 2 μg/mL for **11**; from 0.0624 to 8 μg/mL for **29**). The mean of plasma concentrations (±SE) was calculated and used to estimate the pharmacokinetic parameters by using a noncompartmental model (WinNonlin Enterprise software, Version 4.0.1).

HPLC–fluorimetric analysis and sample quantification were carried out on a System Gold HPLC Systems (Beckman Coulter) coupled with a Shimadzu fluorescence detector (RF-10AXL), fixed at wavelengths of 295 nm (λ_{ex}) and 390 nm (λ_{em}), using 32 Karat Software (Beckman Coulter). A Symmetry C18 column (5 μm, 4.6 × 150 mm, Waters) was used in gradient mode with a flow rate of 1 mL/min. The mobile phase consisted of 20 mM ammonium acetate in water and acetonitrile (75/25) for the elution of **29**. After 20 min, the proportion of acetonitrile was programmed to linearly increase to 90% over 15 min and held for an additional 5 min for the elution of **11**. Then, the percentage of acetonitrile was decreased within 5 min to 25%. For reequilibration of the column, the proportion was subsequently held at this concentration for 20 min.

Acknowledgment. Funding for this study was provided by the Ministero dell'Università e della Ricerca Scientifica e Tecnologica, Rome, Italy.

Supporting Information Available: Experimental procedures for intermediate compounds and elemental analysis results of target derivatives. This material is available free of charge via the Internet at <http://pubs.acs.org>.

References

- Denekamp, J. Angiogenesis, neovascular proliferation and vascular pathophysiology as targets for cancer therapy. *Br. J. Radiol.* **1993**, *66*, 181–196.
- Burrows, F. J.; Thorpe, P. E. Vascular targeting—A new approach to the therapy of solid tumors. *Pharmacol. Ther.* **1994**, *64*, 155–174.
- Siemann, D. W.; Chaplin, D. J.; Horsman, M. R. Vascular-targeting therapies for treatment of malignant disease. *Cancer* **2004**, *100*, 2491–2499.
- Feron, O. Targeting the tumor vascular compartment to improve conventional cancer therapy. *Trends Pharmacol. Sci.* **2004**, *25*, 536–542.
- Murata, R.; Siemann, D. W.; Overgaard, J.; Horsman, M. R. Improved tumor response by combining radiation and the vascular-damaging drug 5,6-dimethylxanthenone-4-acetic acid. *Radiat. Res.* **2001**, *156*, 503–509.
- Horsman, M. R.; Murata, R. Combination of vascular targeting agents with thermal or radiation therapy. *Int. J. Radiat. Oncol. Biol. Phys.* **2002**, *54*, 1518–1523.
- Pedley, R. B.; El-Emir, E.; Flynn, A. A.; Boxer, G. M.; Dearling, J.; Raleigh, J. A.; Hill, S. A.; Stuart, S.; Motha, R.; Begent, R. H. Synergy between vascular targeting agents and antibody-directed therapy. *Int. J. Radiat. Oncol. Biol. Phys.* **2002**, *54*, 1524–1531.
- Wedge, S. R.; Kendrew, J.; Ogilvie, D. J.; Hennequin, L. F.; Brave, S. R.; Ryan, A. J.; Ashton, S. E.; Calvete, J. A.; Blakey, D. C. Combination of the VEGF receptor tyrosine kinase inhibitor ZD6474 and vascular-targeting agent ZD6126 produces an enhanced anti-tumor response. *Proc. Am. Assoc. Cancer Res.* **2002**, *43*, 1081–1083.
- Pettit, G. R.; Cragg, G. M.; Herald, D. L.; Schmidt, J. M.; Lobavanijaya, P. Isolation and structure of combretastatin. *Can. J. Chem.* **1982**, *60*, 1347–1376.
- Hamel, E.; Lin, C. M. Interactions of combretastatin, a new plant-derived antimetabolic agent with tubulin. *Biochem. Pharmacol.* **1983**, *32*, 3864–3867.
- Lin, C. M.; Singh, S. B.; Chu, P. S.; Dempcy, R. O.; Schmidt, J. M.; Pettit, G. R.; Hamel, E. Interactions of tubulin with potent natural and synthetic analogs of the antimetabolic agent combretastatin: A structure–activity study. *Mol. Pharmacol.* **1988**, *34*, 200–208.
- Lin, C. M.; Ho, H. H.; Pettit, G. R. Antimitotic natural products combretastatin A-4 and combretastatin A-2: Studies on the mechanism of their inhibition of the binding of colchicine to tubulin. *Biochemistry* **1989**, *28*, 6984–6991.
- Pettit, G. R.; Singh, S. B.; Hamel, E.; Lin, C. M.; Alberts, D. S.; Garcia-Kendall, D. Isolation and structure of the strong cell growth and tubulin inhibitor combretastatin A-4. *Experientia* **1989**, *45*, 209–211.
- Boye, O.; Bossi, A. In *The Alkaloids*; Bossi, A., Cordell, G. A., Eds.; Academic: New York, 1992; Vol. 41, pp 125–178.
- Griggs, J.; Metcalfe, J. C.; Hesketh, R. Targeting tumour vasculature: The development of combretastatin A4. *Lancet Oncol.* **2001**, *2*, 82–87.
- Chaplin, D. J.; Hill, S. A. The development of Combretastatin A4 phosphate as a vascular targeting agent. *Int. J. Radiat. Oncol. Biol. Phys.* **2002**, *54*, 1491–1496.
- Pettit, G. R.; Temple, C. Jr.; Narayanan, V. L.; Varma, R.; Boyd, M. R.; Renner, G. A.; Bansal, N. Antineoplastic agents 322. Synthesis of combretastatin A-4 prodrugs. *Anti-Cancer Drug Des.* **1995**, *10*, 299–309.
- Hadimani, M. B.; Hua, J.; Jonklaas, M. D.; Kessler, R. J.; Sheng, Y.; Olivares, A.; Tanpure, R. P.; Weiser, A.; Zhang, J.; Edvardsen, K.; Kane, R. R.; Pinney, K. G. Synthesis, in vitro, and in vivo evaluation of phosphate ester derivatives of combretastatin A-4. *Bioorg. Med. Chem. Lett.* **2003**, *13*, 1505–1508.
- Sheng, Y.; Hua, J.; Pinney, K. G.; Garner, C. M.; Kane, R. R.; Prezioso, J. A.; Chaplin, D. J.; Edvardsen, K. Combretastatin family member OX14503 induces tumor vascular collapse through the induction of endothelial apoptosis. *Int. J. Cancer* **2004**, *111* (4), 604–610.
- Nam, N. H. Combretastatin A-4 analogues as antimetabolic antitumor agents. *Curr. Med. Chem.* **2003**, *10*, 1697–1722 and references therein.
- Simoni, D.; Grisolia, G.; Giannini, G.; Roberti, M.; Rondanin, R.; Piccagli, L.; Baruchello, R.; Rossi, R.; Romagnoli, R.; Invidiata, F. P.; Grimaudo, S.; Jung, M. K.; Hamel, E.; Gebbia, N.; Crosta, L.; Abbadessa, V.; Di Cristina, A.; Dusonschet, L.; Meli, M.; Tolomeo, M. Heterocyclic and phenyl double-bond-locked combretastatin analogues possessing potent apoptosis-inducing activity in HL60 and in MDR cell lines. *J. Med. Chem.* **2005**, *48*, 723–736.
- Maya, A. B. S.; Perez-Melero, C.; Mateo, C.; Alonso, D.; Fernandez, J. L.; Gajate, C.; Mollinedo, F.; Pelaez, R.; Caballero, E.; Medarde, M. Further naphthylcombretastatins. An investigation on the role of naphthalene moiety. *J. Med. Chem.* **2005**, *48*, 556–568.
- Flynn, B. L.; Hamel, E.; Jung, M. K. One-pot synthesis of benzo[b]furan and indole inhibitors of tubulin polymerization. *J. Med. Chem.* **2002**, *45*, 2670–2673.
- Pinney, K. G.; Bounds, A. D.; Dingerman, K. M.; Mocharla, V. P.; Pettit, G. P.; Bai, R.; Hamel, H. A new anti-tubulin agent containing the benzo[b]thiophene ring system. *Bioorg. Med. Chem. Lett.* **1999**, *9*, 1081–1086.
- Combretastatin Derivatives with Cytotoxic Action. Patent RM2003A000355. Daniele Simoni, Romeo Romagnoli, Giuseppe Giannini, Domenico Aloatti, Claudio Pisano.
- Howard, T. T.; Lingerfelt, B. M.; Purnell, B. L.; Scott, A. E.; Price, C. A.; Townes, H. M.; McNulty, L.; Handl, H. L.; Summerville, K.; Hudson, S. J.; Bowen, J. P.; Kiakos, K.; Hartley, J. A.; Lee, M. Novel furano analogues of duocarmycin C1 and C2: Design, synthesis, and biological evaluation of *seco*-iso-cyclopropylfuran[2,3-*e*]indoline (*seco*-iso-CFI) and *seco*-cyclopropyltetrahydrofuran[2,3-*f*]quinoline (*seco*-CFQ) analogues. *Bioorg. Med. Chem.* **2002**, *10*, 2941–2952 and references therein.
- Batt, D. G.; Jones, D. G.; La Greca, S. Regioselectivity in the acid-catalyzed isomerization of 2-substituted 1,4-dihydro-1,4-epoxynaphthalenes. *J. Org. Chem.* **1991**, *56*, 6704–6708.
- Horii, Z.; Katagi, T.; Tamura, Y.; Tanaka, T.; Yamawaki, Y. Synthetic studies on Sorigenins. III. Syntheses of 4-methoxynaphtho[2,3-*c*]furan-1(3*H*)-one and 5-methoxynaphtho[1,2-*c*]furan-3(1*H*)-one. *Chem. Pharm. Bull.* **1962**, *10*, 898–901.
- Gabbutt, C. D.; Hepworth, J. D.; Heron, B. M.; Thomas, D. A.; Kilner, C.; Partington, S. M. Synthesis and photochromic properties of methoxy substituted 2,2-diaryl-2*H*-naphtho[1,2-*b*]pyrans. *Heterocycles* **2004**, *63*, 567–582.
- Silverstein, E. M.; Bassler, G. C.; Morrill, T. C. *Spectrometric Identification of Organic Compounds*; John Wiley and Sons: New York, 1981; pp 264–265.
- Pettit, G. R.; Anderson, C. R.; Herald, D. L.; Jung, M. K.; Lee, D. J.; Hamel, E.; Pettit, R. K. Antineoplastic agents. 487. Synthesis and biological evaluation of the antineoplastic agent 3,4-methylenedioxy-5,4'-dimethoxy-3'-amino-*Z*-stilbene and derived amino acid amides. *J. Med. Chem.* **2003**, *46*, 525–531.
- Pettit, G. R.; Moser, B. R.; Boyd, M. R.; Schmidt, J. M.; Pettit, R. K.; Chapuis, J. C. Antineoplastic agents 460. Synthesis of combretastatin A-2 prodrugs. *Anti-Cancer Drug Des.* **2001**, *16*, 185–193.
- Cushman, M.; Nagarathnam, D.; Gopal, D.; Chakraborti, A. K.; Lin, C. M.; Hamel, E. Synthesis and evaluation of stilbene and dihydrostilbene derivatives as potential anticancer agents that inhibit tubulin polymerization. *J. Med. Chem.* **1991**, *34*, 2579–2588.
- Cushman, M.; Nagarathnam, D.; Gopal, D.; He, H.-M.; Lin, C. M.; Hamel, E. Synthesis and evaluation of analogues of (*Z*)-1-(4-methoxyphenyl)-2-(3,4,5-trimethoxyphenyl)ethene as potential cytotoxic and antimetabolic agents. *J. Med. Chem.* **1992**, *35*, 2293–2306.
- Kirwan, I. G.; Loadman, P. M.; Swaine, D. J.; Anthony, D. A.; Pettit, G. R.; Lippert, J. W., III; Shnyder, S. D.; Cooper, P. A.; Bibby, M. C. Comparative preclinical pharmacokinetic and metabolic studies of the combretastatin prodrugs combretastatin A4 phosphate and A1 phosphate. *Clin. Cancer Res.* **2004**, *10*, 1446–1453.
- Folkman, J.; Haudenschild, C. C.; Zetter, B. R. Long-term culture of capillary endothelial cells. *Proc. Natl. Acad. Sci. U.S.A.* **1979**, *76* (10), 5217–5221.
- Skehan, P.; Storeng, R.; Scudiero, D.; Monks, A.; McMahon, J.; Vistica, D.; Warren, J. T.; Bokesch, H.; Kenney, S.; Boyd, M. R.; New colorimetric cytotoxicity assay for anticancer-drug screening. *J. Natl. Cancer Inst.* **1990**, *82* (13), 1107–1112.
- Tahir, S. K.; Han, E. K.-H.; Credo, B.; Jae, H.-S.; Pietenpol, J. A.; Scatena, C. D.; Wu-Wong, J. R.; Frost, D.; Sham, H.; Rosenberg, S. H.; Ng, S.-C. A-204197, a new tubulin-binding agent with antimetabolic activity in tumor cell lines resistant to known microtubule inhibitors. *Cancer Res.* **2001**, *61*, 5480–5485.